

Measurement and prediction of the acoustic performance of poroelastic foam filled mufflers for sleep apnoea devices

Peter Jones and Nicole Kessissoglou

School of Mechanical and Manufacturing Engineering, The University of New South Wales, Sydney NSW 2052, Australia

PACS: 43.50.Gf, 43.55.Ka

ABSTRACT

Mufflers are incorporated into continuous positive airway pressure (CPAP) devices to reduce noise in the air paths to and from the flow generating fan. The mufflers are very small, irregularly shaped and are required to attenuate noise up to 10 kHz. The acoustic performance of these predominantly reactive mufflers can be enhanced with the inclusion of dissipative materials. It is important that the acoustic performance of these mufflers is reliably predicted and optimised, in order to improve the user experience and maximise compliance with the CPAP therapy. In this study, the acoustic properties of two polyurethane foams were determined using a two-cavity method. Acoustic models of two muffler designs, having dimensions similar to those used in CPAP devices and incorporating foam-filled regions, have been developed using a commercial finite element analysis software package. Experimental results for the mufflers have been obtained using the two-microphone acoustic pulse method. Results of the transmission loss of the muffler designs obtained from the finite element models are presented and validation of the computational results is discussed.

INTRODUCTION

Obstructive sleep apnoea (OSA) is a medical condition that can be successfully managed through the application of a positive pressure to the airway. This elevated airway pressure is produced by a flow generating fan within a continuous positive airway pressure (CPAP) device. Noise from the flow generator is controlled using mufflers situated in the flow path at the fan inlet and the flow generator outlet. The mufflers are very small, are often irregularly shaped and are required to attenuate noise up to 10 kHz. They are predominantly reactive however dissipative materials are often incorporated into the design to enhance the acoustic performance. This study builds on previous work by the authors [1,2] on acoustic finite element (FE) modelling of reactive CPAP muffler designs. The acoustic characteristics of two polyurethane foams were obtained experimentally and the corresponding properties incorporated into FE models of two muffler designs. Results of the transmission loss of the foam-filled mufflers obtained from the FE models are presented. Validation of the computational results is discussed using data obtained using a two-microphone acoustic pulse experimental measuring technique.

MUFFLER DESIGNS

Two muffler designs were selected for analysis. The first design consists of a simple cylindrical expansion chamber having dimensions similar to those used in CPAP devices. The foam insert occupies the full volume of the expansion chamber. The second design (Fig. 1a) is that of a production CPAP muffler which, while geometrically complex, consists

of a single chamber having coaxial inlet and outlet ports located at one end of the chamber.

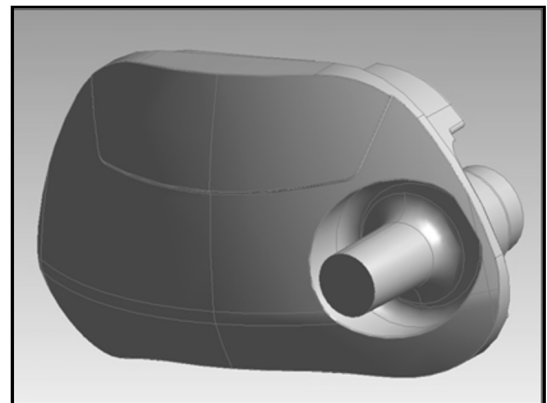


Figure 1a. CPAP muffler design

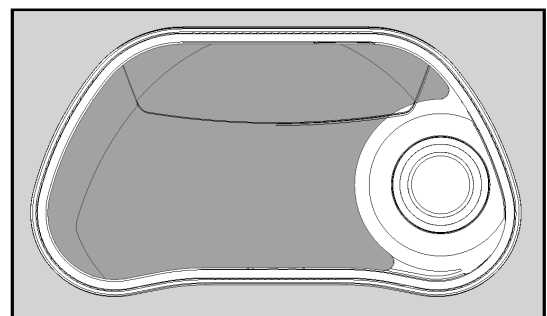


Figure 1b. CPAP muffler foam insert

The foam insert, shown by the grey shaded area in Fig. 1b, occupies the majority of the chamber volume. It is important to note that, unlike the foam insert in the first muffler design, this insert does not intrude into the direct path between the inlet and outlet ports.

Two different polyurethane foam materials were selected for comparison and are shown in Table 1. The first foam is a material currently being used in CPAP muffler designs while the second is a material which is more likely to be used in protective packaging and is unlikely to be recommended for acoustic applications. The latter was chosen for inclusion in the assessment as it was anticipated that the acoustic properties would be sufficiently dissimilar to the first to provide an instructive comparison.

Table 1. Polyurethane foam physical properties

Foam	Description	Density (kg/m ³)
A	Acoustic (light grey)	33.9
B	Non-acoustic (dark grey)	23.2

FOAM MODELLING METHOD

Characteristic impedance (Z_c) and propagation coefficient (γ) of porous materials can be presented as simple power-law functions by [3,4]:

$$Z_c = \rho_{air} c_{air} \left[1 + C_1 \left(\frac{\rho_{air} f}{r_o} \right)^{C_2} - j * C_3 \left(\frac{\rho_{air} f}{r_o} \right)^{C_4} \right] \quad (1)$$

$$\gamma = (\omega / c_{air}) \left[C_5 \left(\frac{\rho_{air} f}{r_o} \right)^{C_6} + j \left(1 + C_7 \left(\frac{\rho_{air} f}{r_o} \right)^{C_8} \right) \right] \quad (2)$$

where ρ_{air} and c_{air} are respectively the density and speed of sound in air, f is the frequency and r_o is the airflow resistivity. Delany and Bazley obtained values for the coefficients C_1 to C_8 using a range of fibrous absorbent materials [3]. Several authors have noted that predictions made using Delany and Bazley's original coefficients are not especially accurate when applied to poroelastic materials and have obtained different coefficients [5-8]. In this work, the characteristic impedance, propagation coefficient and airflow resistivity of the two foams summarised in Table 1 were measured experimentally. The methodology described by Delany and Bazley was then applied to derive the unknown coefficients C_1 to C_8 for these particular foams. Once the coefficients have been determined and substituted back into Eqs. (1) and (2), the resulting equations are then suitable for incorporating directly into the finite element model. They may also be used to gain some insight into the acoustic performance of the foams by re-stating them in terms of an equivalent fluid having a complex speed of sound (c_B) and complex mean density (ρ_B) by [9]:

$$c_B = \frac{j\omega}{\gamma}, \quad c_B = \left[\frac{\omega\beta}{(\alpha^2 + \beta^2)} \right] + j \left[\frac{\omega\alpha}{(\alpha^2 + \beta^2)} \right] \quad (3)$$

$$\rho_B = \frac{Z_c}{c_B}, \quad \rho_B = \left[\frac{X\alpha + R\beta}{\omega} \right] - j \left[\frac{R\alpha - X\beta}{\omega} \right] \quad (4)$$

where $Z_c = R + jX$ and $\gamma = \alpha + j\beta$.

EXPERIMENTAL METHODS

Three experimental methods are presented in what follows. The first two methods are used to obtain the characteristic impedance, propagation constant and flow resistivity of the foams. The third method is used to measure the transmission loss of the mufflers.

Characteristic impedance and propagation constant

The characteristic impedance and propagation constant of porous materials can be measured by applying the transfer function method to a two-cavity approach [10]. A sample of homogeneous porous material is positioned within an impedance tube and against the front face of a moveable plunger. The plunger is then withdrawn away from the sample, producing an air cavity with a known depth between the rear face of the sample and the plunger (Fig. 2).

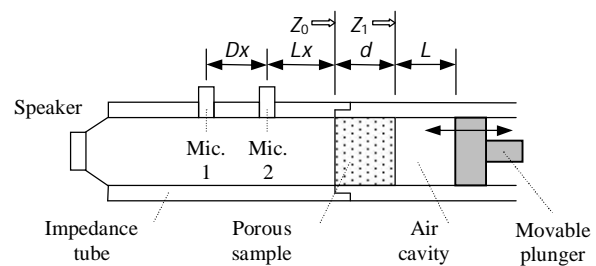


Figure 2. Schematic diagram of the impedance tube configuration

The normal surface acoustic impedance of a sample was measured in accordance with ISO 10534 [12] with an air cavity depth L . A random signal was fed to the loudspeaker of a Brüel & Kjær Type 4206 impedance tube. The transfer function H_{12} from microphone position 1 to position 2, defined by the complex ratio p_2/p_1 , was measured using a two channel Fast Fourier transform. The surface acoustic impedance Z_0 is then obtained by [13]:

$$Z_0 = jZ_{air} \left\{ \frac{H_{12} \sin[k(Lx + Dx)] - \sin(kLx)}{\cos(kLx) - H_{12} \cos[k(Lx + Dx)]} \right\} \quad (5)$$

The impedance tube plunger was withdrawn a further distance and the measurement procedure was repeated at depth L' to obtain Z'_0 . The theoretical impedances of a closed tube with depth L and L' are given by [10]:

$$Z_1 = -jZ_{air} \cot(kL), \quad Z'_1 = -jZ_{air} \cot(kL') \quad (6,7)$$

where k is the wave number and Z_{air} ($= \rho_{air} c_{air}$) is the characteristic impedance of air. The characteristic impedance and propagation constant of the material can then be calculated by [10]:

$$Z_c = \pm \sqrt{\frac{Z_0 Z'_0 (Z_1 - Z'_1) - Z_1 Z'_1 (Z_0 - Z'_0)}{(Z_1 - Z'_1) - (Z_0 - Z'_0)}} \quad (8)$$

$$\gamma = \left(\frac{1}{2d} \right) \ln \left(\frac{Z_0 + Z_c}{Z_0 - Z_c} \right) \left(\frac{Z_1 - Z_c}{Z_1 + Z_c} \right) \quad (9)$$

where the sign in Eq. (8) is selected so that the real part of Z_c is positive.

Airflow resistivity

The airflow resistivity of a homogeneous material is given by $r_o = \Delta P / du$, where ΔP is the static pressure drop across the material, d is the unit thickness and u is the linear velocity of air passing through it [14]. Measurements were performed according to the direct airflow method described in ISO 9053 [14]. A unidirectional airflow was passed through cylindrical samples having 25mm thickness and 100mm diameter (see Fig. 3) and the resulting pressure drop between the two free faces of the sample was measured.

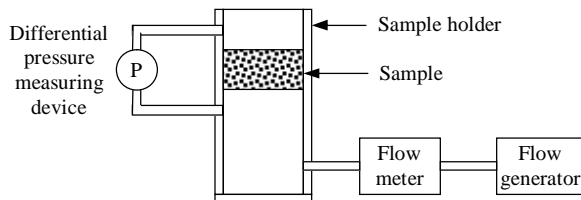


Figure 3. Schematic diagram of the airflow resistivity experimental set-up

Transmission loss

Figure 4 shows a schematic diagram of the two-microphone experimental set-up used in the current work. A transient acoustic pulse was generated from a Brüel & Kjær LAN-XI Pulse front end and fed to two horn drivers via a power amplifier.

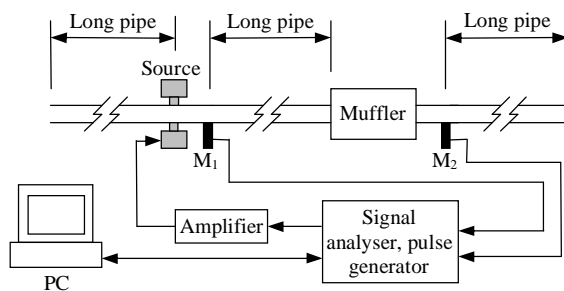


Figure 4. Schematic diagram of the two-microphone acoustic pulse experimental set-up

The pulse propagated down the 18mm diameter conduit where it was measured by the upstream microphone, M_1 , before continuing to the muffler inlet. The pressure of the corresponding pulse transmitted from the outlet of the muffler was measured by the downstream microphone, M_2 . Rectangular windowing with leading and trailing cosine tapers was applied to the time history measured by M_1 and exponential windowing with a leading cosine taper and 5ms decay constant (τ) was applied to the time history measured by M_2 . Utilising long lengths of pipe in the system provided sufficient time delay (approximately 19ms) between the arrival of the initial pulse and the reflected waves generated at the muffler and pipe ends to facilitate extraction of the initial positive travelling wave. These extracted time histories were captured for 100 individual pulses with the results averaged in the time domain prior to being Fourier transformed. The transmission loss for the muffler was then obtained using Eq. (10).

$$TL = 10 \log_{10} \left(\frac{FFT_1}{FFT_2} \right) \quad (10)$$

FFT_1 and FFT_2 are the (power) autospectra of the Fourier transformed time histories of the incident and transmitted waves, respectively.

FINITE ELEMENT MODELS

Acoustic finite element models of each of the muffler designs were developed using the commercially available finite element analysis (FEA) package COMSOL (version 3.5a). The muffler models were meshed using Lagrange-quadratic elements with controls applied to produce a mesh having at least 6 elements per acoustic wavelength at the upper bound of the frequency range being analysed (limiting case). A harmonic pressure of 1 Pa was specified at the inlet and a radiation condition applied at inlet and outlet. The air was assumed to be non-flowing and inviscid and acoustic damping was not applied at the fluid-structure interface. The foam inserts were modelled using the Delany-Bazley formulation described earlier and having parameters that were obtained experimentally for each of the foam types using the methods described in the previous section. Transmission loss is calculated directly in COMSOL using the acoustic power at the inlet and outlet of the acoustic system.

RESULTS AND DISCUSSION

The results are presented in three sub-sections corresponding to the foam airflow resistivity measurements, foam acoustic property measurements (characteristic impedance and propagation constant) and the muffler transmission loss measurements, respectively.

Foam airflow resistivity

Airflow resistivity for each foam type was measured according to the direct airflow method described in ISO 9053. Data was also recorded at linear airflow velocities greater than the 4 mm/s upper limit recommended by the Standard to ascertain the effect of turbulent flow on the apparent airflow resistivity for the foams being studied. The values for airflow resistivity calculated using data within the laminar range are presented in Table 2 and it can be seen that the measured airflow resistivity of the two foam types is significantly different. This is consistent with the observed surface pore sizes and spacing.

Figure 5 shows that the apparent airflow resistivity for the light grey foam increases as the linear airflow is increased beyond the laminar region, while the apparent airflow resistivity of the dark grey foam remains largely unaffected. This difference in observed behaviour is significant as the Delany-Bazley method uses a single value for flow resistivity to characterise the porous material.

Table 2. Foam airflow resistivity

Foam	Description	Flow resistivity (Rayls/m)	95% confidence (Rayls/m)
A	Acoustic (light grey)	8,445	182
B	Non-acoustic (dark grey)	2,652	36

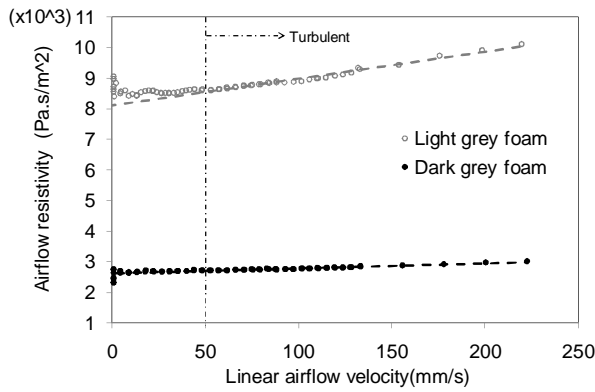


Figure 5. Airflow resistivity of dark and light grey foams

Foam acoustic properties

The normal surface impedance for each foam type was measured and calculated using the test method described in ISO 10534. Measurements were obtained at four cavity depths – 25mm, 50mm, 75mm, and 100mm – using samples having 25mm thickness. The characteristic impedance and propagation constant were calculated for each of the cavity combinations 25mm/50mm, 50mm/75mm and 75mm/100mm using Eqs. (11) and (12) and the results for the three combinations were averaged. Equations (1) and (2) can be restated as:

$$\log_{10} \frac{R}{\rho_{air} c_{air}} - 1 = C_2 \log_{10} \left(\frac{\rho_{air} f}{r_o} \right) + \log_{10}(C_1) \quad (11)$$

$$\log_{10} \left(\frac{-X}{\rho_{air} c_{air}} \right) = C_4 \log_{10} \left(\frac{\rho_{air} f}{r_o} \right) + \log_{10}(C_3) \quad (12)$$

$$\log_{10} \left(\frac{\alpha c_{air}}{\omega} \right) = C_6 \log_{10} \left(\frac{\rho_{air} f}{r_o} \right) + \log_{10}(C_5) \quad (13)$$

$$\log_{10} \left(\frac{\beta c_{air}}{\omega} - 1 \right) = C_8 \log_{10} \left(\frac{\rho_{air} f}{r_o} \right) + \log_{10}(C_7) \quad (14)$$

As Eqs. (11) to (14) are of the form $y = mx + b$, it is possible to obtain the equation coefficients by fitting linear trend lines through the experimental data. The coefficients that were obtained are presented in Table 2 alongside Delany and Bazley’s original coefficients. It can be seen that the coefficients for each of the two foam types are significantly different from each other and also from the original Delany-Bazley coefficients, with the exception of the attenuation constant (α) which shows reasonable agreement. These differences support previous findings that predictions made using the original Delany-Bazley coefficients are not especially accurate when applied to poroelastic materials [5-8]. However it is worth noting that the propagation constant of both foam types correlate well with the flow resistivity, producing correlation coefficients between 0.96 and 0.99. The characteristic impedance of the light grey foam also correlates well, producing correlation coefficients between 0.88 and 0.92. These observations are consistent with the findings of Wu [6] who reported correlation coefficients between 0.85 and 0.99 for porous plastic open-celled foams. While the correlation coefficients for the characteristic impedance of the dark grey foam are less encouraging (0.58 and 0.72), examination of the characteristic impedance curves shows significant departure from linear behaviour at

frequencies greater than 1,600Hz. This suggests that the observed behaviour might be attributed to sample preparation as this frequency coincides with the transition between measurements obtained in the 100mm diameter impedance tube and those obtained in the 29mm diameter impedance tube.

The Delany-Bazley relationships are only considered to be valid over the range $0.012 \leq (\rho_{air} f / r_o) \leq 1.2$ [4]. Assuming an air density of 1.18 kg/m^3 , the valid frequency range for the dark grey foam is 25 Hz to 2,690 Hz, while for the light grey foam it is 85 Hz to 8,500 Hz.

Table 2. Delany-Bazley equation coefficients

Equation coefficient	Dark grey foam	Light grey foam	Delany-Bazley
C_1	0.2051	0.2824	0.0571
C_2	-0.2249	-0.3659	-0.7540
C_3	0.1175	0.0980	0.0870
C_4	-0.4851	-0.6144	-0.7320
C_5	0.2039	0.1692	0.1890
C_6	-0.5416	-0.5728	-0.5950
C_7	0.2688	0.2561	0.0978
C_8	-0.3111	-0.4657	-0.7000

Equations (3) and (4) were used to obtain the complex speed of sound and complex density of the light grey foam based on the coefficients in Table 2. The results for the complex speed of sound and density are shown in Figs. 6 and 7, respectively. A similar exercise has not been performed for the dark grey foam due to (a) concerns over the integrity of the data and (b) the reduced valid frequency range. The Delany-Bazley model shows excellent agreement with the experimental data. This is not unexpected as the model coefficients were derived using the same set of experimental data and the correlation coefficients were good.

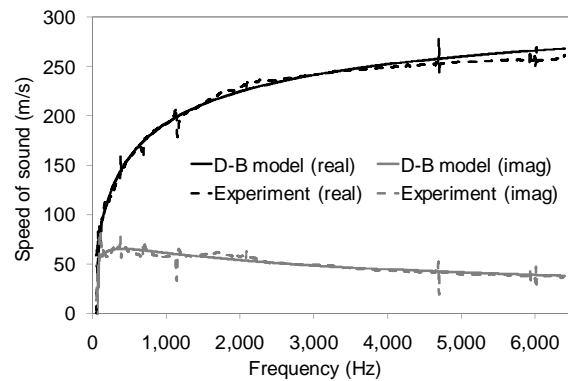


Figure 6. Equivalent fluid speed of sound of light grey foam

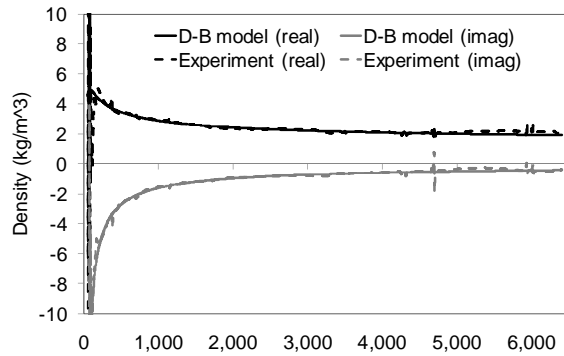


Figure 7. Equivalent fluid density of light grey foam

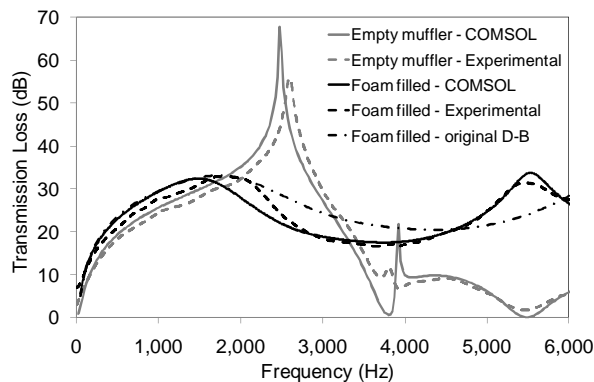


Figure 8. Transmission loss results for a cylindrical expansion chamber muffler with and without light grey foam, comparing COMSOL results using derived D-B parameters (solid lines) and original D-B parameters (dash-dot lines) and experimental results (dashed lines)

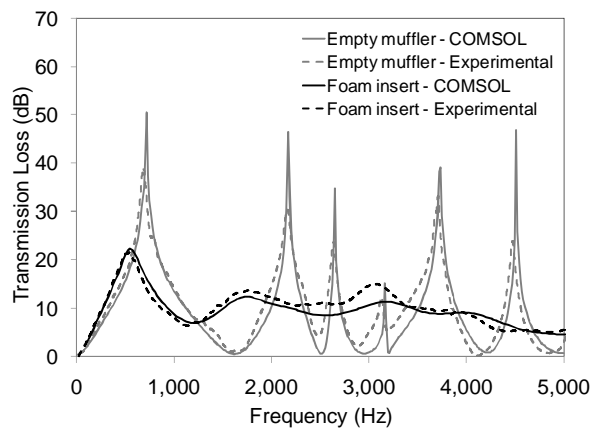


Figure 9. Transmission loss results for a CPAP muffler with and without light grey foam, comparing COMSOL results (solid lines) and experimental results (dashed lines)

Muffler transmission loss

Figures 8 and 9 compare the transmission loss results obtained using the COMSOL finite element model with results obtained experimentally, for the cylindrical expansion chamber muffler and CPAP chamber muffler, respectively. Both figures show excellent agreement over the frequency range assessed, both with and without the foam insert. In Fig. 8, the FE analysis was repeated using the measured

airflow resistivity in combination with the original Delany-Bazley equation coefficients. This model only achieves a good match with the experimental data up to 1,600 Hz and also fails to produce the broad peak centred at 5,500 Hz. The results in Fig. 9 complement those obtained for the cylindrical expansion chamber muffler (Fig. 8) as the foam insert is located off to one side of the chamber in this design and plane waves from the inlet duct are not required to pass through the foam before exiting the muffler chamber.

CONCLUSIONS

The characteristic impedance and propagation constant of two polyurethane foams have been determined experimentally using a two-cavity impedance tube method. Airflow resistivity of the two foams has been determined experimentally using the direct airflow method described in ISO 9053. Acoustic models of two muffler designs having dimensions similar to those used in CPAP devices and incorporating foam-filled regions have been developed using a commercial finite element analysis software package. Transmission loss results for the mufflers have been experimentally obtained using the two-microphone acoustic pulse method.

The magnitudes of the airflow resistivity measured for each of the two foam types are significantly different and they also exhibit differing sensitivity to linear airflow variations. The Delany-Bazley equation coefficients calculated for each of the two foam types differ from the original Delany-Bazley coefficients and also from each other. As the original Delany-Bazley model assumes a single value for flow resistivity to characterise the porous material and applies a fixed set of equation coefficients to model all porous materials, use of the original Delany-Bazley model to represent these foams will lead to inaccurate predictions.

Transmission loss results for both muffler designs with and without the foam inserts were presented. The transmission loss results obtained computationally incorporated the derived Delany-Bazley coefficients. Excellent agreement between the numerical and experimental results was obtained across the entire considered frequency range. By characterising foam as an equivalent fluid using straight-forward airflow resistivity and impedance tube measurements, it has been shown that accurate predictions of the acoustic performance of foam inserts can be achieved using finite element modelling.

ACKNOWLEDGEMENTS

Financial assistance for this work was provided as part of an ARC Linkage Project jointly funded by the Australian Research Council and ResMed.

REFERENCES

- 1 P.W. Jones and N.J. Kessissoglou "An evaluation of current commercial acoustic FEA software for modelling small complex muffler geometries: Prediction vs Experiment", *Proceedings of ACOUSTICS 2009*, Adelaide, Australia, 23-25 November 2009
- 2 P.W. Jones and N.J. Kessissoglou "A numerical and experimental study of the transmission loss of mufflers used in respiratory medical devices", *Acoustics Australia*, **38**(1), 13-19 (2010)
- 3 M.E. Delany and E.N. Bazley "Acoustical properties of fibrous absorbent materials", *Applied Acoustics*, **3**, 105-116 (1970)

- 4 D.A. Bies, and C.H. Hansen, "Flow resistance information for acoustical design", *Applied Acoustics*, **13**, 37-391 (1980)
- 5 I.P. Dunn and W.A. Davern "Calculation of acoustic impedance of multi-layer absorbers", *Applied Acoustics*, **19**, 321-334 (1986)
- 6 Wu Qunli "Empirical Relations between Acoustical Properties and Flow Resistivity of Porous Plastic Open-Cell Foam", *Applied Acoustics*, **25**, 141-148 (1988)
- 7 Y. Miki "Acoustical properties of porous materials – Modifications of Delany-Bazley models", *Journal of the Acoustical Society of Japan*, **11**(1), 19-28 (1990)
- 8 M.K. Ling "Technical Note – Impedance of Polyurethane Foams", *Applied Acoustics*, **34**, 221-224 (1991)
- 9 O.Z. Mehdizadeh and M. Paraschivoiu "A three dimensional finite element approach for predicting the transmission loss in mufflers and silencers with no mean flow", *Applied Acoustics*, **66**, 902-918 (2005)
- 10 H. Utsuno, T. Tanaka, T. Fujikawa and A.F. Seybert, "Transfer function method for measuring characteristic impedance and propagation constant of porous materials", *Journal of the Acoustical Society of America*, **86**(2), 637-643 (1989)
- 11 C. Zwikker and C. Kosten *Sound Absorbing Materials* (Elsevier, New York, 1949)
- 12 *ISO 10534-2:1998: Acoustics – Determination of sound absorption coefficient and impedance in impedance tubes – Part 2: Transfer-function method* (International Organisation for Standardization, Switzerland, 1998)
- 13 M.L. Munjal and A.G. Doige, "The two-microphone method incorporating the effects of mean flow and acoustic damping", *Journal of Sound and Vibration*, **137**(1), 135-138 (1990)
- 14 *ISO 9053:1991: Acoustics – Materials for acoustical applications – Determination of airflow resistance* (International Organisation for Standardization, Switzerland, 1991)
- 15 *C 522-03: Standard Test Method for Airflow Resistance of Acoustical Materials* (ASTM International, United States, 2003)
- 16 A.F. Seybert and D.F. Ross "Experimental determination of acoustic properties using a two-microphone random excitation technique", *Journal of the Acoustical Society of America*, **61**(5), 1362-1370 (1977)
- 17 D.R. Reynolds, *Engineering Principles of Acoustics* (Allyn and Bacon, Massachusetts, 1981)
- 18 A. Barber, *Handbook of Noise and Vibration Control (6th Ed.)* (Elsevier Advanced Technology, Oxford, 1992) p317